and $NF_2\cdot$ are considerably more reactive[28,29] toward addition than is the simple amino radical. In both $PH_2\cdot$ and $NF_2\cdot$ (though for somewhat different reasons) the nonbonding electron density at their respective heavy atoms is expected to be substantially lower than for $NH_2\cdot$ itself. Consequently the repulsive interaction between the nonbonding electrons of these species and the double bond of the olefinic center is undoubtedly diminished relative to the case of simple amino additions; the resulting decrease in the slope of the N potential curve (Figure 5) quite naturally leads to a reduction in the activation energy for such processes and hence to the observed increase in reactivity. This interpretation in turn suggests strongly that the transition state for amino additions is destabilized by electron-donating substituents, in apparent contrast to the behavior of its counterpart in hydrogen abstraction reactions.[4,5]

(28) A. R. Stiles, F. F. Rust, and W. E. Vaughan, *J. Amer. Chem. Soc.*, 74, 3282 (1952); G. M. Burch, H. Goldwhite, and R. N. Haszeldine, *J. Chem. Soc.*, 1083 (1963).
(29) A. J. Dijkstra, J. A. Kerr, and A. F. Trotman-Dickenson, *J. Chem. Soc. A*, 105 (1967).

Acknowledgment. Two of us are most appreciative of the hospitality shown them during their stay in the Department of Chemistry of the University of Nebraska (S. D. P.) and at the Institut für Physikalische Chemie of the University of Mainz (S. S.), respectively. The services and computer time made available by the University of Nebraska and the University of Mainz Computing Centers have been invaluable in this study; the financial support of the Deutsche Forschungsgemeinschaft is gratefully acknowledged.

A Kinetic Study of the Proton Hydrate $H^+(H_2O)_n$ Equilibria in the Gas Phase

A. J. Cunningham, J. D. Payzant, and P. Kebarle*

Contribution from the Department of Chemistry, University of Alberta, Edmonton, Alberta, Canada. *Received March 27, 1972*

Abstract: The kinetics of the gas-phase reactions $H^+(H_2O)_{n-1} + H_2O + M = H^+(H_2O)_n + M$ were studied in a pulsed electron beam high pressure mass spectrometer. The major gas used was methane at a few Torr. Some runs were also made with propane. Water pressures were between 1 and 200 mTorr and temperatures up to ~900°K were used. The kinetics of the approach to the equilibria and the equilibria could be observed under these conditions. The rate constants for the forward and reverse reactions of the lower equilibria were determined at different temperatures. The temperature dependence of the equilibrium constants was used for the evaluation of the $\Delta H^\circ_{n-1,n}$ and $\Delta G^\circ_{n-1,n}$. The present results were found to be in fair agreement with earlier determinations from this laboratory but differ drastically with chemical ionization measurements of Beggs and Field.[1]

A mass spectrometric study of the ions present in air at near atmospheric pressures (~100 Torr) undertaken some 10 years ago led to the accidental observation[2,3] of the proton hydrates $H^+(H_2O)_n$ formed by ion-molecule reactions involving traces of water vapor. The observation of clusters such as $NH_4^+(NH_3)_n$-$(H_2O)_n$, $H^+(CH_3OH)_n$, etc., in ammonia, methanol, and other gases led to the systematic study of ion–solvent molecule interactions and ion equilibria in the gas phase.[4] Measurement of ionic equilibria and their temperature dependence leads to important thermochemical information. For example, determination of the equilibrium constant $K_{n-1,n}$ at suitable temperatures

$$H^+(H_2O)_{n-1} + H_2O = H^+(H_2O)_n \qquad (n-1,n)$$

$$K_{n-1,n} = [H^+(H_2O)_n]/[H^+(H_2O)_{n-1}][H_2O]$$

leads to the determination of $\Delta G^\circ_{n-1,n}$, $\Delta H^\circ_{n-1,n}$, and $\Delta S^\circ_{n-1,n}$ for the stepwise hydration of the proton. Measurement of ion equilibria in the gas phase is useful not only in the study of ion–solvent molecule interactions. The ion-equilibrium method is quite general and has been used in this and other laboratories for the determination of important thermochemical quantities: electron affinities,[5] switching reaction,[6] gas-phase acidities and basicities,[7] H bonding to negative ions,[8] etc. It is to be expected that future equilibrium measurements will provide a large store of data of fundamental interest to many fields of chemistry. Ion-molecule reaction equilibria are generally observed in the presence of reactions by which the ionic charge is destroyed, *i.e.*, positive-negative charge recombination and discharge by diffusion to the wall. Therefore in order to study ion equilibria one must work under conditions where the equilibrium reactions are faster than the other processes. Also the ion sampling method may create problems. Because of these inherent difficulties,

(1) (a) D. P. Beggs and F. H. Field, *J. Amer. Chem. Soc.*, 93, 1567 (1971); (b) F. H. Field and D. P. Beggs, *ibid.*, 93, 1576 (1971).
(2) P. Kebarle and E. W. Godbole, *J. Chem. Phys.*, 39, 1131 (1963).
(3) Attachment of water molecules to the hydrogen ion had been mass spectrometrically observed earlier in flames [P. F. Knewstubb and T. M. Sugden, *Proc. Roy. Soc., Ser. A*, 255, 520 (1960)], field emission [H. D. Beckey, *Z. Naturforsch. A*, 15, 822 (1960)], and gas discharges [P. F. Knewstubb and A. W. Tickner, *J. Chem. Phys.*, 38, 464 (1963)].
(4) P. Kebarle, "Ions and Ion Pairs in Organic Reactions," M. Szwarc, Ed., Wiley, New York, N. Y., 1972, Chapter 2, and "Ion Molecule Reactions," J. L. Franklin, Ed., Plenum Press, New York, N. Y., 1972, Chapter 7.
(5) J. L. Pack and A. V. Phelps, *J. Chem. Phys.*, 44, 1870 (1966).
(6) N. G. Adams, D. K. Bohme, D. B. Dunkin, F. C. Fehsenfeld, and E. E. Ferguson, *ibid.*, 52, 3133 (1970).
(7) J. P. Briggs, R. Yamdagni, and P. Kebarle, *J. Amer. Chem. Soc.*, submitted for publication.
(8) R. Yamdagni and P. Kebarle, *ibid.*, 93, 7139 (1971).

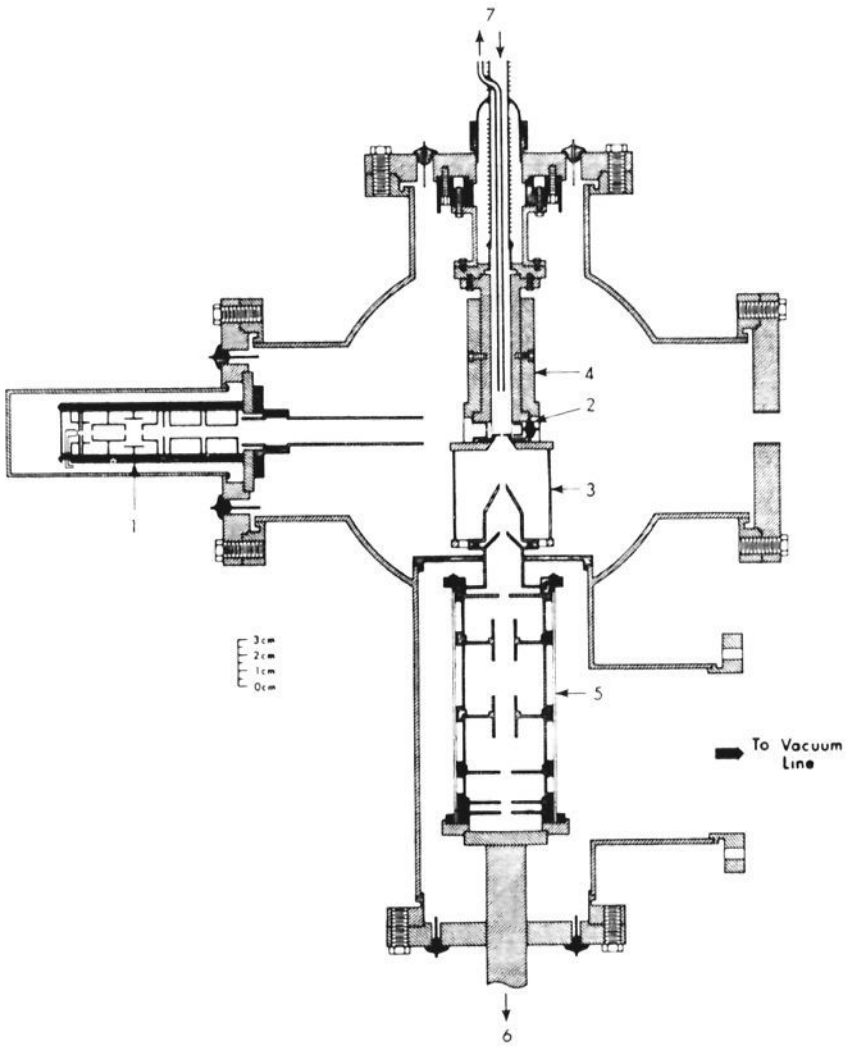

Figure 1. Apparatus: (1) electron gun assembly, (2) ion source in ion source block, (3) bottom lid of ion source and electrostatic shielding mesh, (4) outer mantle of ion source with heater wells and heaters, (5) ion acceleration tower, (6) to magnetic mass analysis, (7) slow flow circulation gas supply to ion source.

some objections to the ion equilibria studies were raised by Friedman and coworkers.[9,10]

More recently Field and coworkers[1] have published studies dealing with ion equilibria in general and the proton hydrate equilibria $(n,n-1)$ in particular. The results obtained by Field are in vast disagreement with measurements obtained in this laboratory.[11] Field's value for $K_{1,2}$ (at 300°K)[1b] is more than ten orders of magnitude smaller than the value obtained in this laboratory.[11] Since the proton hydrates were among the first equilibria measurements conducted in this laboratory and since considerable refinements in experimental technique have been made, we decided to repeat the determinations. The present results include kinetic studies which permit determinations of the rate constants of the forward and reverse reactions and their temperature dependence. Furthermore several runs were made under conditions similar to those used by Field in order to establish the cause of the large differences.

Experimental Section

The ion-molecule reaction ion source and mass spectrometer are similar to those described earlier[5] and incorporate modifications mentioned in more recent publications.[6,7] Therefore only a brief description of the apparatus and procedures will be given here.

Methane gas at pressures of 3–4 Torr containing known pressures of water (1–200 mTorr) was flowed (~0.3 l. sec^{-1} at 4 Torr) through the stainless steel ion source (see Figure 1). Ionization was obtained with 2000-V electrons produced in an electron gun and entering the ion source through a narrow slit (12 μ × 2 mm). The electron beam was pulsed "on" for 10 μsec and "off" for 6 msec. Each pulse contained some 10^6 electrons. The ions react with other molecules as they diffuse through the field free ion source. Some of the ions come to the vicinity of the molecular flow ion exit slit, (12 μ × 2 mm, razor blade edges) escape through the leak into the evacuated region (10^{-4} Torr), and are subjected to mass analysis (15-cm radius, 90° tube) and electron multiplier detection. The multiplier pulses are collected in a multiscaler whose 6-msec sweep is triggered by the electron beam "on" pulse. In most runs, the dwell time per channel was 20 μsec. By repeatedly pulsing (~10^4 pulses) the electron gun the temporal profile of an ion could be obtained. The time-of-flight of ions outside the ion source (~10 μsec) is short compared to the residence time in the ion source. Correction for the time of flight of different mass was obtained with a pulse delay circuit.

Considerable care was taken in order to obtain uniform temperature in the ion source and ion exit slit. A thermocouple embedded deep in the ion source block and close to the inner wall of the ion source was used for measurement of the ion source temperature. Block heaters were installed not only around the ion source but also in the bottom plate (electrostatic shield electrode) (see Figure 1). The temperature of this section was monitored by separate thermocouples.

The water pressure in the ion source was determined by "weight loss" measurements. In a series of runs water vapor was added to the carrier gas (CH_4) stream by a thermostated capillary connected to a thermostated small glass bulb containing liquid water. The weight loss of water from the bulb, combined with the measured flow rate of the carrier gas, allowed one to determine the partial pressure of the water in the carrier stream. It was assumed that the minor component H_2O and the carrier gas travel at the same speed. A plot of the partial pressure of water in the carrier gas *vs.* $(P_1^2 - P_2^2)$, where P_1 is the vapor pressure of the thermostated water in the bulb and P_2 is the carrier gas pressure, gave a straight line going through the origin as required by the relationship for viscous flow. In some runs pure water was used whose pressure was determined with a capacitance micromanometer.

Results and Discussion

(A) General Results and Kinetic Measurements. Most of the measurements were done with methane at a known pressure between 3 and 4 Torr and water at pressures between 1 and 200 mTorr. Some experiments were done with ethane and propane as major gases and some with pure water. The use of a major gas was dictated by two considerations. First it was intended to work with reaction systems similar to those used by Field[1] in order to obtain more comparable results. Secondly, the presence of a third (dilutant) gas is necessary for the kinetic studies[12] and the equilibrium measurements.

The principle ions formed by the ionization and ion-molecule reactions in methane are CH_5^+ and $C_2H_5^+$. Both of these ions react with water[1] producing H_3O^+. The H_3O^+ then forms the higher hydrates by the reactions $n-1,n$.

$$H_3O^+ + H_2O + M = H^+(H_2O)_2 + M \quad (1,2)$$

$$H^+(H_2O)_2 + H_2O + M = H^+(H_2O)_3 + M \quad (2,3)$$

$$H^+(H_2O)_{n-1} + H_2O + M = H^+(H_2O)_n + M \quad (n-1,n)$$

M is the third body, *i.e.*, the major gas required for the deactivation of the initially excited association product and for the activation of $H^+(H_2O)_n$ in the decomposition reactions $n,n-1$. The clustering reactions are expected[12] to be third order in the forward direction

(9) M. DePaz, J. J. Leventhal, and L. Friedman, *J. Chem. Phys.*, **51**, 3748 (1969).

(10) A reply to Friedman's paper is contained in P. Kebarle, *ibid.*, **53**, 2129 (1970). This is followed by comments by L. Friedman, *ibid.*, **53**, 2130 (1970).

(11) P. Kebarle, S. K. Searles, A. Zolla, J. Scarborough, and M. Arshadi, *J. Amer. Chem. Soc.*, **89**, 6393 (1967).

(12) A. Good, D. A. Durden, and P. Kebarle, *J. Chem. Phys.*, **52**, 212 (1970).

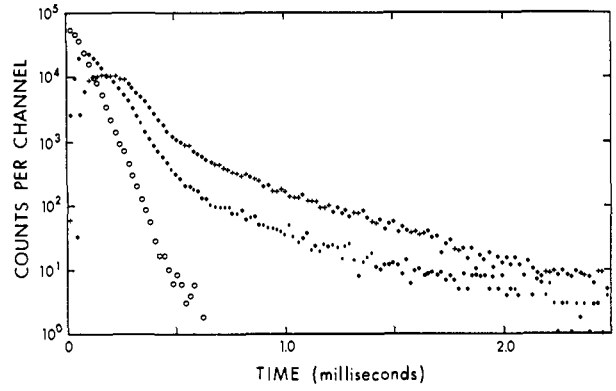

Figure 2. Time dependence of ion counts observed with multiscaler: CH_4, 3.55 Torr; H_2O, 3.22 mTorr, 125°. (○) H_3O^+, (●) $H^+(H_2O)_2$, (+) $H^+(H_2O)_3$. Sequence $H_3O^+ \rightarrow H^+(H_2O)_2 \rightleftarrows H^+(H_2O)_3$ is easily observed. The equilibrium appears as a constant difference in the log of the ion counts.

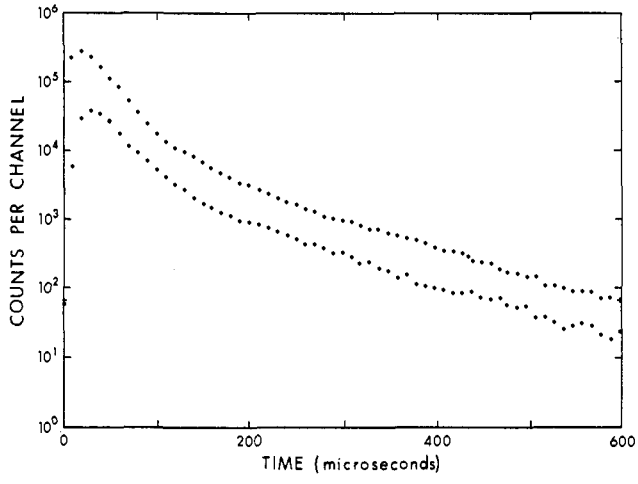

Figure 3. Time dependence of ion counts with rapid achievement of $H_3O^+ \rightleftarrows H^+(H_2O)_2$ equilibrium: CH_4, 4.0 Torr; H_2O, 99.7 mTorr, 518°. (+) H_3O^+, (●) $H^+(H_2O)_2$.

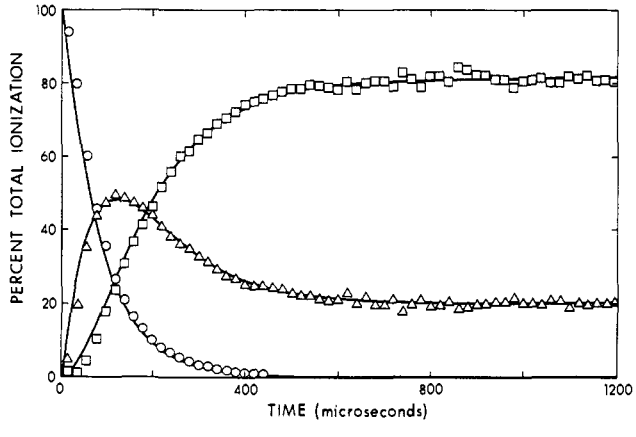

Figure 4. Results of experiment shown in Figure 2 but presented in per cent of total ionization: (○) H_3O^+, (△) $H^+(H_2O)_2$, (□) $H^+(H_2O)_3$. Solid lines connecting experimental points are analog computer calculated concentrations of reaction system.

$(n-1,n)$ and second order in the reverse $(n,n-1)$ direction at pressures below 10 Torr.

The time dependence of the ion counts obtained in a typical run is shown in Figure 2. The intensities of all ions decrease with time after the ionizing pulse. This

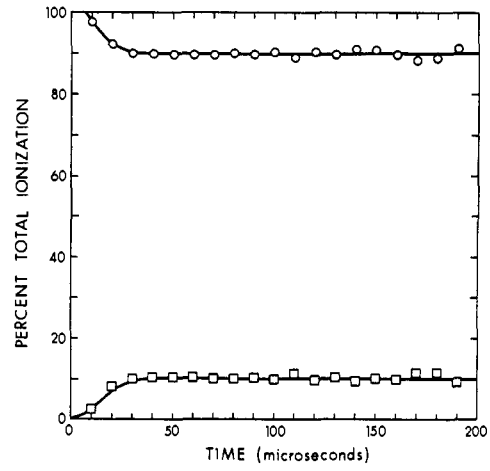

Figure 5a. H_3O^+–$H^+(H_2O_2)$ equilibria at different conditions: (○) H_3O^+, (□) $H^+(H_2O)_2$; 4 Torr at CH_4, 47 mTorr of H_2O, 533°.

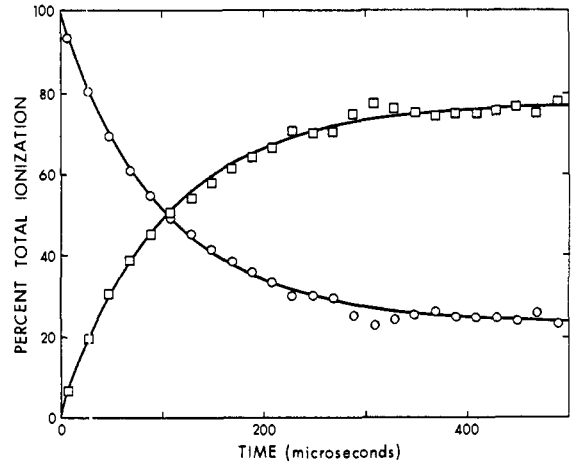

Figure 5b. (○) H_3O^+, (□) $H^+(H_2O)_2$; 6 Torr of CH_4, 27 mTorr of H_2O, 399°. Note that more than 400 μsec is required for the achievement of equilibrium when the H_2O pressure is 27 mTorr.

decrease is due to diffusion of ions to the wall followed by discharge on the wall. Overlayed on this decrease are the changes due to ion-molecule reactions. The sequence $H_3O^+ \rightarrow H^+(H_2O)_2 \rightleftarrows H^+(H_2O)_3$ can be easily deduced. Thus H_3O^+ disappears rapidly; the $H^+(H_2O)_2$ intensity increases and then decreases due to the formation of $H^+(H_2O)_3$. The achievement of equilibrium becomes noticeable at longer times where (the logarithmic) intensities become parallel; *i.e.*, the intensity ratios become constant. The initial ion-molecule reactions by which CH_5^+ and $C_2H_5^+$ are formed and the formation of H_3O^+ by reactions of these ions with H_2O are too fast to be observed under the conditions used.

A simpler kinetic sequence leading to rapid equilibrium between H_3O^+ and $H^+(H_2O)_2$ is shown in Figure 3. The log plots are seen to be parallel over most of the observed range. The high water concentration used in this experiment leads to rapid equilibrium in the clustering reactions. Only $H^+(H_2O)_2$ is formed since the higher clusters are unstable at the high ion source temperature used.

A more convenient display of the data is obtained through a normalization procedure initiated in earlier work.[12] Normalized ion counts at time t are obtained

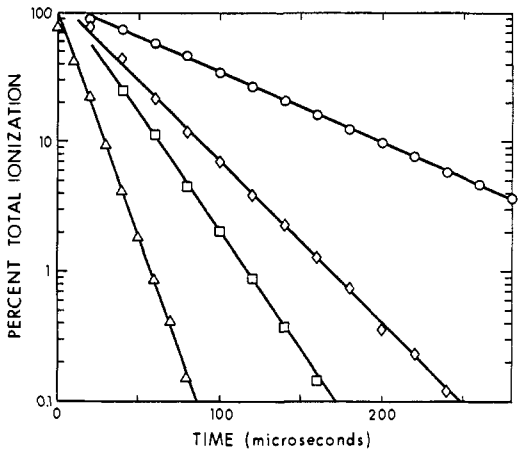

Figure 6. Logarithmic plots of normalized H_3O^+ intensity with time. Slope provides pseudo-first-order rate constant $\nu_1 = k_1 \cdot [H_2O][CH_4]$: (△) 25.5, (□) 13, (◇) 7, (○) 3:2 mTorr of H_2O, 4 Torr of CH_4, 125°.

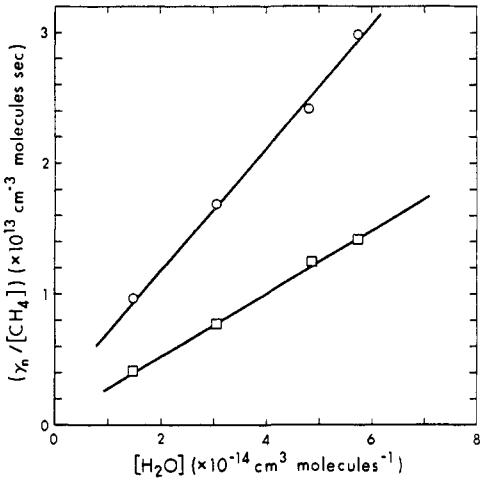

Figure 7. Dependence of pseudo-first-order rate constant $\nu_1 = k_1[H_2O][CH_4]$ on water concentration. (○) $\nu_1/[CH_4]$, (□) $\nu_2/[CH_4]$, 223°.

by dividing the ion count of a given ion by the ion count for all ions (*i.e.*, the total ionization). Such normalized ion-time dependencies are given in Figures 4 and 5 for the runs shown in Figures 2 and 3. The data in Figures 4 and 5 will be treated as if they represented ion concentration changes in a reaction vessel in which the total ion concentration is constant with time.

We may call the forward reaction rate constants for 1,2 and 2,3 k_1 and k_2, etc., and the reverse reactions k_{-1}, k_{-2}, etc. In a given run the concentrations of the neutrals are constant and the ion-molecule reactions are all (pseudo) first order. The pseudo-first-order rate constants (reaction frequencies) are $\nu_1 = k_1[H_2O] \cdot [M]$, $\nu_{-1} = k_{-1}[M]$, etc. The ν's were determined by fitting computer generated concentration–time curves to the experimentally determined time dependence. The solid lines in Figures 4 and 5 are such computer curves. Figure 4 illustrates that very satisfactory fits can be obtained even for more involved reaction sequences. The computer calculated concentrations were obtained by programming an analog computer to reproduce the reaction system 1,2, 2,3, etc. The ν's were treated as variable parameters and changed until a best fit of the experimental points was obtained.

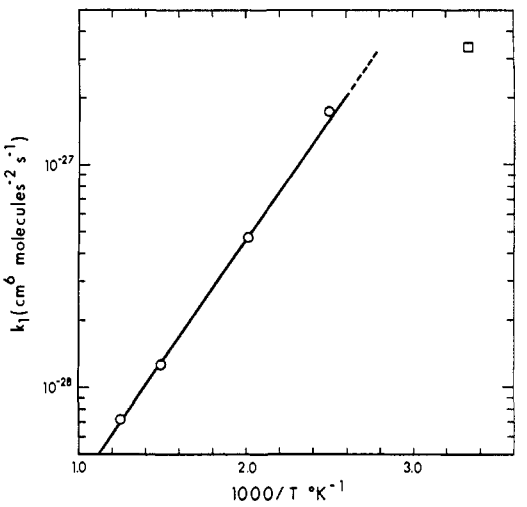

Figure 8. Temperature dependence of third-order rate constant k_1 for reaction $H_3O^+ + H_2O + CH_4 = H^+(H_2O)_2 + CH_4$. Arrhenius-type plot leads to negative "activation energy" of 4.9 kcal/mol: (○) third-body CH_4; (□) third body N_2; see ref 12.

The ν_1 values could also be determined without the aid of the computer by selecting conditions under which essentially all H_3O^+ disappeared by reaction and plotting then the logarithm of the normalized H_3O^+ intensity *vs.* time. Such plots are shown in Figure 6. The slopes of the straight lines obtained are equal to $\nu_1/2.3$. The log plots (Figure 6) include more points (those at long t) than the computer fits. Virtually identical ν_1 values were obtained by both methods.

Figure 7 shows plots of $\nu_n/[CH_4]$ plotted *vs.* $[H_2O]$ for $n = 1, 2$. The slopes of the straight lines obtained should be equal to the rate constants k_1 and k_2. Similar data for the reverse reactions were also obtained. Determinations such as those described above were done at several temperatures. At higher temperatures only k_1 (and k_{-1}) could be determined with accuracy since the equilibrium concentrations of the $H^+(H_2O)_3$ cluster becomes too small for satisfactory observation. Figure 8 shows the temperature dependence of k_1. Third-order rate constants for termolecular reactions such as k_1 are known to decrease with increasing temperature. We have used an Arrhenius-type plot even though the resulting "activation" energy (which is negative) has no explicit physical meaning. It is interesting to note that k_1 which is $\sim 14 \times 10^{-27}$ at 300°K decreases to 7×10^{-29} at 830°K, *i.e.*, by a factor of 200. This is a very substantial decrease which leads to a negative "activation" energy of ~5 kcal/mol. An earlier determination of k_1 with N_2 as third body is also shown in Figure 8. The N_2 rate constant is lower by a factor of ~3. A higher third body efficiency for methane is to be expected.

The reverse rate constants k_{-1}, k_{-2}, etc., can be determined from the forward rate constants and the equilibrium constants by the relationship $K_{n-1,n} = k_n/k_{-n}$. The rate data obtained in the present work are summarized in Table I.

Some runs were made with 4 Torr of propane as the major gas. The principle ion series observed in this case was $C_3H_7^+(H_2O)_n$. The propyl hydrates were also observed by Field.[1b] The proton hydrates formed the second most important series of ions, but many other apparently pure hydrocarbon ions were also

Table I. Temperature Dependence of the Proton Hydration Reactions $H_3O^+ + H_2O + CH_4 \underset{k_{-1}}{\overset{k_1}{\rightleftharpoons}} H^+(H_2O)_2 + CH_4$

Temp, °K	k_1[a]	k_2[a]	k_3[a]	k_{-1}[b]	k_{-2}[b]	k_{-3}[b]	K_{12}[d]	K_{23}[d]	K_{34}[d]
296	1.35 (−26)[c]			5.4 (−25)[c]			8.0 (14)[c]		
398	1.34 (−27)	0.98 (−27)	0.42 (−27)	3.20 (−20)[c]	1.90 (−14)	2.13 (−12)	1.02 (9)[c]	1240	4.75
496	4.64 (−28)	2.2 (−28)		1.97 (−17)[c]	5.4 (−13)		4.6 (5)[c]	7.9	
672	1.71 (−28)			2.78 (−14)			112		
805	7.15 (−29)			3.9 (−13)			2.2		

[a] k_1, k_2, k_3, units of $cm^6\ sec^{-1}$. [b] k_{-1}, k_{-2}, k_{-3}, units of $cm^3\ sec^{-1}$. [c] Extrapolated value. [d] $K_{1,2}$, $K_{2,3}$, $K_{3,4}$, standard state 1 Torr.

Table II. Thermochemical Data for $H^+(H_2O)_{n-1} + H_2O = H^+(H_2O)_n$ Equilibria

	$-\Delta H^\circ_{n-1,n}$,[a] kcal/mol				$-\Delta G^\circ_{n-1,n}$, kcal/mol[b]			
	This laboratory		Beggs and Field		This laboratory		Beggs and Field	
$n-1,n$	A	B	C	D	A	B	C	D
1,2	31.6	36	7	16.3	24.3	25	7.7	11.2
2,3	19.5	22.3	13	14.8	13.0	13.6	9.3	9.7
3,4	17.5	17	16.8	17.6	9.3	8.5	8.4	8.6
4,8	[c]				[c]			

[a] A, present work (CH_4 as major gas); B, this laboratory[11] (H_2O as major gas, Ar as major gas); C, Beggs and Field[1a] (CH_4 as major gas); D, Beggs and Field[1b] (C_3H_8 as major gas). [b] Standard state 1 atm, 300°K. A and B values extrapolated to 300° from van't Hoff plots of equilibrium constants obtained at higher temperature (see Figure 9). [c] For data on higher equilibria up to $n = 8$ see ref 11.

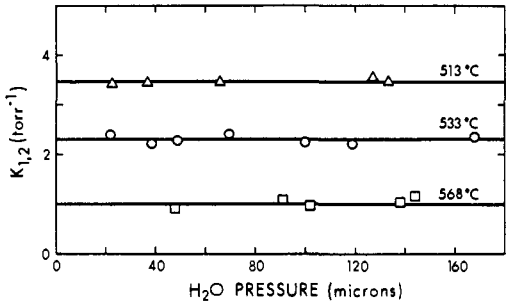

Figure 9. Equilibrium constant $K_{1,2}$ at several temperatures plotted *vs.* water pressure.

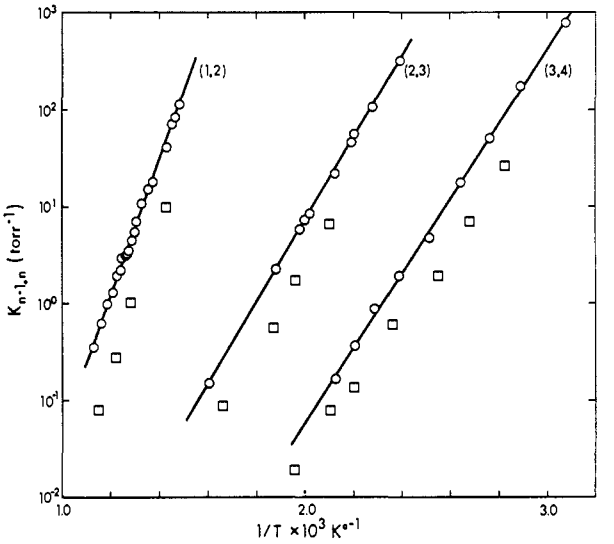

Figure 10. van't Hoff plots of equilibrium constants $K_{n-1,n}$ for $H^+(H_2O)_{n-1} + H_2O = H^+(H_2O)_n$ equilibria. Comparison with earlier determination[11] from this laboratory done partly with pure water and partly with argon as major gas: (○) present work, (□) earlier determination.

present. Thus a large intensity was observed at mass 86 probably corresponding to $C_6H_{14}^+$. The proton hydrate intensities at long reaction time led to equilibrium constants which were equal, within experimental error, to those observed with methane. The propane system was not subjected to detailed study since being rather complex it was less convenient to use.

(B) Temperature Dependence of the Hydration Equilibria. The equilibrium constants for the hydrations $n-1,n$ were determined from the concentration ratios of the ions $n-1$ and n observed at long reaction times where the ion ratio had become time independent, indicating that equilibrium had been achieved (Figure 5). Increasing the water concentration at a fixed temperature and constant major gas (CH_4) pressure allowed one to establish that the equilibrium constants are independent of the water concentration. Results of such runs are shown in Figure 9 for the 1,2 equilibrium at three different temperatures. The data show that an increase of water pressure from about 20 to 160 mTorr leaves the equilibrium constants unchanged. Similar results were obtained also for the 2,3 and 3,4 equilibria.

The van't Hoff plots of the equilibrium constants are shown in Figure 10. Included in the figure are also the experimental points obtained in the earlier determination[11] done in this laboratory. The plots involving the 4,5 equilibria are not shown since for these there was essentially complete agreement between the present and earlier results. The enthalpy and free energy values resulting from the present and earlier measurements are summarized in Table II. It is evident from Figure 9 that there is a fair agreement between the present and earlier results. Unfortunately the agreement is not as good as we had hoped. Thus the present equilibrium constants are higher by a factor of about 3.5 for the (1,2), 3 for the (2,3), and 2.5 for the (3,4) equilibria.

In general differences up to a factor of 2 can be attributed to inaccuracies in the measurement of water pressure (especially when water is added as a minor component), temperature, errors due to the method of sampling, mass discrimination effects in the mass spectrometer, etc. Since the present results are in agreement with the earlier measurements for the 4,5 equilib-

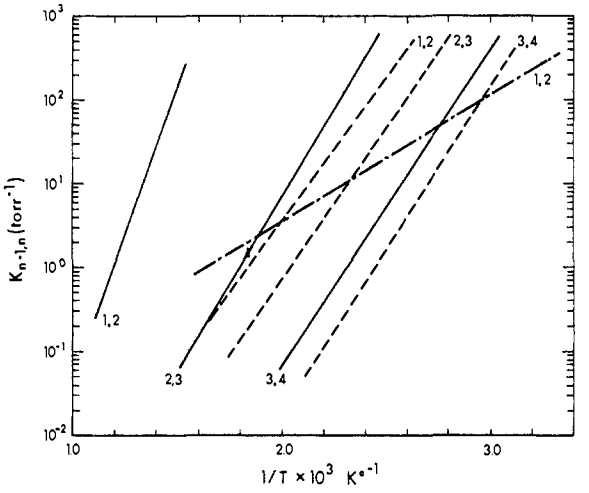

Figure 11. Comparison of van't Hoff plots from present work with those obtained by Beggs and Field:[1] (——) present work; (– – –) Beggs and Field, propane as major gas; (–·–·–) Beggs and Field, methane as major gas. Note large discrepancy between 1,2 plot from present results and two completely different 1,2 plots of Beggs and Field.

ria measured at room temperature and since the discrepancy tends to increase with temperature it was considered that errors in temperature determinations were the most likely major contributing factor. The 1,2 equilibria was measured at temperatures as high as 900°K, and here an error of 20° can lead to a twofold variation in the determined equilibrium constants. The difficulty arises because of temperature control and measurement problems near the ion exit slit which is by necessity thin walled.

Accordingly, a detailed study of the influence of the temperature distribution in the vicinity of the ion exit slit on the proton hydrate equilibria was undertaken. Heaters embedded in the electrostatic shield electrode (see Figure 1) allowed equilibrium constant determinations with the shield temperature less than, equal to, or greater than the ion source temperature. Under each of these three temperature conditions excellent agreement with the data shown in Figure 10 was observed. Disagreement with the less numerous earlier data from this laboratory probably reflects an error in temperature determination in the previous studies when no special precautions were undertaken to ensure a controlled temperature region close to the ion exit slit.

The new enthalpies are somewhat lower than those reported previously. $\Delta H_{2,1}$ = 31.6 *vs.* 36 kcal/mol of the earlier determination, $\Delta H_{3,2}$ = 19.6 *vs.* 22.3, and $\Delta H_{4,3}$ = 17.5 *vs.* 17. Again the largest difference is for the 2,1 equilibrium which was measured at the highest temperature.

The experimental determinations of the water cluster dissociation energies based on collisional detachment studies by DePaz, Leventhal, and Friedman[9] are in general agreement with the $\Delta H_{n,n-1}$ values from this laboratory. Theoretical calculations of the dissociation energy $D(H_3O^+-H_2O) \approx \Delta H_{2,1}$ by Kraemer and Diercksen,[13] Kollman and Allen,[14] and Newton and Ehrenson[15] lead to the values 32.2, 35, and 37 kcal/mol, respectively. These values are in the same range as the results from the present laboratory.

The data obtained by Beggs and Field[1] are compared with results from this laboratory in Figure 11 and Table II. There exists fair agreement for the higher equilibria[1] including the 3,4 reaction. However, there is very serious disagreement between the results for the 2,3 and particularly the 1,2 equilibrium.

The temperature range used by Beggs and Field for the 1,2 equilibrium determinations centers at about 125°. The time-dependent concentration changes displayed in Figure 4 show the H_3O^+ being completely converted to $H^+(H_2O)_2$ and higher hydrates for a water pressure of 3.2 mTorr and 125°. The H_3O^+–$H^+(H_2O)_2$ equilibrium is observed only at much higher temperatures, *i.e.*, above 350° (Figure 5). Unfortunately the highest temperature explored by Beggs and Field[1b] was only 255°. Examining the van't Hoff plot given by Beggs and Field (Figure 3, ref 1b) one finds that all the $K_{1,2}$ equilibrium constants for temperatures below ~160°, which corresponds to over half of the temperature range covered, were obtained with a constant water pressure of 0.7 mTorr. Using k_1 = 1.34 × 10^{-27} (Table I, 125°) which is in the right range for clustering reactions of this type,[12,16] one calculates a half-life for conversion of H_3O^+ to $H^+(H_2O)_2$ of about 1000 μsec (1 Torr of methane, 0.7 mTorr of H_2O). The ion residence time in Field's source according to his own estimate[1] is only 10–30 μsec, strongly suggesting that his measurements were obtained prior to the establishment of equilibrium.[17] We are therefore unable to rationalize the linearity of his van't Hoff plot and the resultant $\Delta H_{2,1}$ value of 16.3 kcal/mol.[1b]

(13) W. P. Kraemer and G. H. F. Diercksen, *Chem. Phys. Lett.*, **5** 463 (1970).
(14) P. A. Kollman and L. C. Allen, *J. Amer. Chem. Soc.*, **92**, 6101 (1970).
(15) M. D. Newton and S. Ehrenson, *ibid.*, **93**, 4971 (1971).
(16) F. C. Fehsenfeld, M. Mosesman, and E. E. Ferguson, *J. Chem. Phys.*, **55**, 2115, 2120 (1971); L. J. Puckett and M. W. Teague, *ibid.*, **54**, 2564 (1971).
(17) NOTE ADDED IN PROOF. The remarks contained in this paragraph should be equally valid also for a more recent publication: S. L. Bennett and F. H. Field, *J. Amer. Chem. Soc.*, **94**, 5186 (1972), published after the present work had been submitted for publication.